RESEARCH ARTICLE

WILEY

Gas-foamed poly(lactide-co-glycolide) and poly(lactide-co-glycolide) with bioactive glass fibres demonstrate insufficient bone repair in lapine osteochondral defects

Eve Salonius[1] [ORCID] | Virpi Muhonen[1] | Kalle Lehto[2] | Elina Järvinen[1] | Tuomo Pyhältö[3] | Markus Hannula[2] | Antti S. Aula[2,4] | Peter Uppstu[5] | Anne-Marie Haaparanta[2] | Ari Rosling[5] | Minna Kellomäki[2] | Ilkka Kiviranta[1,3]

[1] Department of Orthopaedics and Traumatology, Clinicum, Faculty of Medicine, University of Helsinki, Helsinki, Finland

[2] Department of Electronics and Communications Engineering, Tampere University of Technology, BioMediTech, Institute of Biosciences and Medical Technology, Tampere, Finland

[3] Department of Orthopaedics and Traumatology, Helsinki University Hospital, Helsinki, Finland

[4] Department of Medical Physics, Imaging Centre, Tampere University Hospital, Tampere, Finland

[5] Laboratory of Polymer Technology, Centre of Excellence in Functional Materials at Biological Interfaces, Åbo Akademi University, Turku, Finland

Correspondence
Ilkka Kiviranta, Department of Orthopaedics and Traumatology, Institute of Clinical Medicine, University of Helsinki, Haartmaninkatu 8, 00290, Helsinki, Finland.
Email: ilkka.kiviranta@helsinki.fi

Funding information
Tekes, Grant/Award Number: 3110/31/08

Abstract

Deep osteochondral defects may leave voids in the subchondral bone, increasing the risk of joint structure collapse. To ensure a stable foundation for the cartilage repair, bone grafts can be used for filling these defects. Poly(lactide-co-glycolide) (PLGA) is a biodegradable material that improves bone healing and supports bone matrix deposition. We compared the reparative capacity of two investigative macroporous PLGA-based biomaterials with two commercially available bone graft substitutes in the bony part of an intra-articular bone defect created in the lapine femur. New Zealand white rabbits ($n = 40$) were randomized into five groups. The defects, 4 mm in diameter and 8 mm deep, were filled with neat PLGA; a composite material combining PLGA and bioactive glass fibres (PLGA–BGf); commercial beta-tricalcium phosphate (β-TCP) granules; or commercial bioactive glass (BG) granules. The fifth group was left untreated for spontaneous repair. After three months, the repair tissue was evaluated with X-ray microtomography and histology. Relative values comparing the operated knee with its contralateral control were calculated. The relative bone volume fraction ($\Delta BV/TV$) was largest in the β-TCP group ($p \leq 0.012$), which also showed the most abundant osteoid. BG resulted in improved bone formation, whereas defects in the PLGA–BGf group were filled with fibrous tissue. Repair with PLGA did not differ from spontaneous repair. The PLGA, PLGA–BGf, and spontaneous groups showed thicker and sparser trabeculae than the commercial controls. We conclude that bone repair with β-TCP and BG granules was satisfactory, whereas the investigational PLGA-based materials were only as good as or worse than spontaneous repair.

KEYWORDS

animal model, biomaterial, bone repair, intra-articular, poly(lactide-co-glycolide)

1 | INTRODUCTION

Joint trauma may lead to deep osteochondral defects with severe subchondral bone loss (van Dijk, Reilingh, Zengerink, & van Bergen, 2010). The impairment of joint biomechanics and tissue metabolism leads to dysfunction of the joint and increases the risk of posttraumatic osteoarthritis and collapse of the joint structure (McKinley, Borrelli, D'Lima, Furman, & Giannoudis, 2010). These can lead to pain, swelling, and restricted movement of the joint (Jackson, Lalor, Aberman, & Simon, 2001).

Due to the poor intrinsic repair capacity of cartilage and osteoarthritis as the potential consequence of cartilage lesions, various

treatment options have been developed to preserve joints after damage (Huey, Hu, & Athanasiou, 2012). The current surgical methods to treat osteochondral defects include autologous osteochondral transfer, fresh osteochondral allografts, autologous chondrocyte implantation, and arthroplasty (Seo, Mahapatra, Singh, Knowles, & Kim, 2014). The choice of a treatment option depends on the size, depth, and location of the lesion as well as the age and previous treatments of the patient.

In intra-articular bone fractures and deep osteochondral defects, both the articular cartilage and the underlying bone should be taken into consideration when choosing the treatment method (Mano & Reis, 2007). Large bone voids should be filled with bone grafts to provide the healing defect site with sufficient structural support, which is a prerequisite for a successful cartilage repair. Autografts are the gold standard of bone grafting. Due to the limited availability, donor site morbidity, pain, and risk of infection and nerve injury (Arrington, Smith, Chambers, Bucknell, & Davino, 1996), allografts harvested from a cadaver have been used as an alternative source. However, allografts are associated with the risk of immune reaction and disease transmission. Tissue-engineered substitutes have been developed to overcome these limitations (Oryan, Alidadi, Moshiri, & Maffulli, 2014).

An advantageous bone filler that could be used together with a cartilage reparative construct remains to be developed. An optimal bone filler in a deep osteochondral defect would provide the tissue with mechanical support, be able to function as a carrier for reparative cells, degrade gradually as neotissue forms, and enable cartilage reparation (Oryan et al., 2014).

Several biomaterials have been studied for bone applications. Bioceramics, calcium phosphates, such as osteoconductive beta-tricalcium phosphate (β-TCP), have been used in clinical practice for over 20 years (Ghazal, Prein, & Müller, 1992; Stahl & Froum, 1986). β-TCP resorbs by osteoclastic activity and is replaced by new bone *in vivo* (Eggli, Muller, & Schenk, 1988). Friability and a limited osteogenic effect are the main problems encountered with β-TCP (Liu & Lun, 2012). Bioactive glasses (BGs) are silica-based materials that promote bone formation and have been in clinical use since the 1980s (Brauer, 2015; Keranen et al., 2011). Some BGs have shown antibacterial properties, thus mitigating the risk of surgical infections (Lindfors et al., 2010). BGs, like β-TCP, are brittle, and thus their mechanical properties are limited (Jones, 2013).

Bioabsorbable polymers have been actively studied as bone filler materials. Aliphatic polyesters of alpha-hydroxy acids are the most commonly used, and poly(lactide-co-glycolide) (PLGA) is often favoured in regenerative medicine due to its biocompatibility, relatively rapid and controllable degradation, and existing approval for clinical use by the U.S. Food and Drug Administration (Gentile, Chiono, Carmagnola, & Hatton, 2014,Serino, Rao, Iezzi, & Piattelli, 2008). Three-dimensional scaffolds made of PLGA have been shown to support cell attachment and bone matrix deposition on the scaffold surface and to promote bone healing compared with spontaneous repair (Karp, Shoichet, & Davies, 2003; Kleinschmidt, Marden, Kent, Quigley, & Hollinger, 1993). The acidic by-products that form during the degradation process as well as poor mechanical strength are the main limitations of synthetic polymers (Garcia-Gareta, Coathup, & Blunn, 2015).

Results of the use of porous PLGA scaffolds in the repair of bone defects have been promising (Pan et al., 2015). In our preliminary study in rats (unpublished), there was an island-like bone formation inside the implanted PLGA in the absence of inflammatory cells. Thus, we hypothesized that a porous plug-like PLGA rod could meet the requirements for a bone filler in osteochondral defects. We produced a cylindrical scaffold by gas foaming (CO_2) PLGA to be tested *in vivo* in a rabbit model.

Although polymer scaffolds are biocompatible, they lack sufficient bioactivity (Zeimaran et al., 2015). As BG has shown osteoconductive properties (Gunn, Rekola, Hirvonen, & Aho, 2013), we hypothesized that combining PLGA with bioactive glass fibres (BGf) would enhance the regenerative capacity of the biomaterial. Therefore, we also produced a rod-formed composite material combining PLGA with BGf in a freeze-drying process.

The purpose of this study was to evaluate the potential of two investigational PLGA-based biomaterials against two commercial biomaterials, and lesions left without treatment, in the repair of the bony part of deep osteochondral defects in a rabbit model.

2 | MATERIALS AND METHODS

A total of 40 female New Zealand white rabbits were obtained from a commercial supplier (Harlan Laboratories B.V., Venray, the Netherlands). The animals were 18 weeks old. They were housed in individual cages, acclimatized for 1 week before the operations, and their wellbeing was observed daily. The study was authorized by the Finnish National Animal Experiment Board (ESAVI/3785/04.10.03/2011) and conducted according to the ethical guidelines and regulations of the Finnish Act on Animal Experimentation (62/2006). The rabbits were randomized into five groups (*n* = 8 in each group). Four groups received PLGA, PLGA–BGf, commercial BG, or commercial β-TCP as a bone substitute material (Figure 1a). The fifth group was an untreated control group (spontaneous), which did not receive any bone substitute material.

2.1 | Preparation of the biomaterials

PLGA polymers were produced at Åbo Akademi University. Medical grade monomers of D-lactide and glycolide were acquired from Corbion (Corbion Purac, Gorinchem, the Netherlands) and L-lactide from Futerro (Escanaffles, Spain). The PLGA was polymerized in an argon atmosphere by ring-opening polymerization with 0.1mol-% stannous octoate as initiator and a molecular weight determining amount of 1-decanol as coinitiator. After polymerization, the polymer was purified by dissolution in dichloromethane and precipitation in ethanol. The PLGA had a lactide to glycolide ratio of 7:3 with equal amounts of D- and L-lactide and a weight average molecular weight of 48 000 g/mol.

PLGA scaffolds were produced at Åbo Akademi University with the gas foaming method. PLGA was first extruded into approximately 2.8 mm thick rods, which were cut to 16-mm long pieces. The PLGA pieces were then placed in custom-made Teflon molds with an inner diameter of 4.0 mm. The molds were placed in a chamber with a
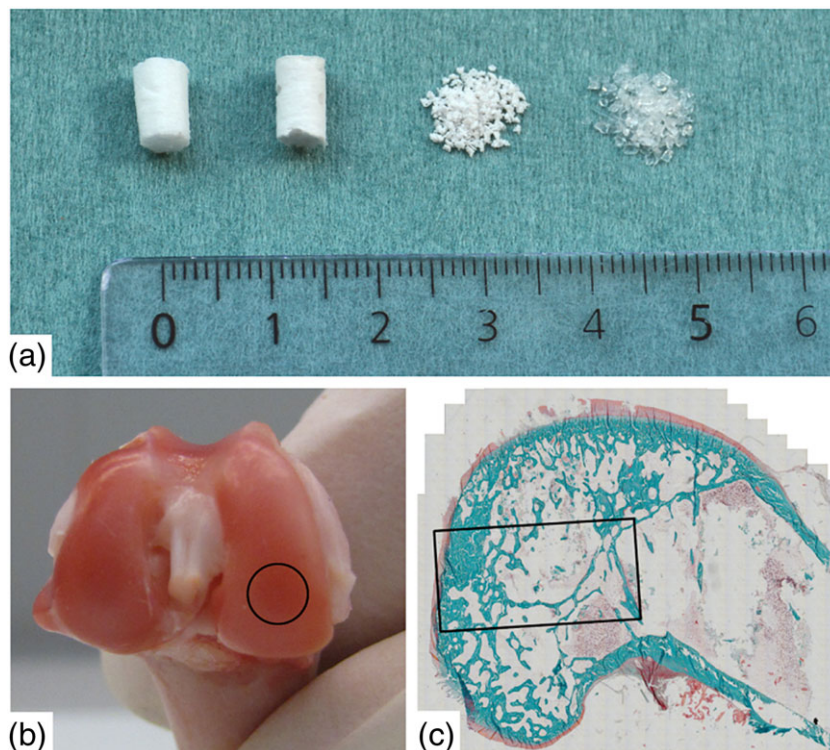
FIGURE 1 (a) A photograph of all the investigated bone substitutes from left to right: poly(lactide-co-glycolide) (PLGA), poly(lactide-co-glycolide)–bioactive glass fibres (PLGA–BGf), beta-tricalcium phosphate (β-TCP), and bioactive glass (BG). The site of the defect in the medial condyle of the femur (b) and its depth into the bone tissue (c) are indicated with a black line [Colour figure can be viewed at wileyonlinelibrary.com]

carbon dioxide pressure of 55 bar for 10 hr, then the pressure was released rapidly in 5 s. The rods were to some extent soft with a porosity of over 90%, which consisted of mainly closed pores. Scaffolds with the length of 8 mm and a mass of 24–27 mg were then cut from the foamed rods and sterilized with gamma irradiation with a dose of 25 kGy.

The PLGA–BGf composites were produced at Tampere University of Technology. Bioresorbable melt-derived glass fibres (Vivoxid Ltd., Turku, Finland), denoted as BGf, were composed of 68.6 SiO_2, 12.5 Na_2O, 9.3 CaO, 7.2 MgO, 1.8 B_2O_3, and 0.6 P_2O_5 (in mol-%). The average fibre diameter was 13 μm. The BGf was cut into staple fibres of approximately 10 cm in length and carded into mesh. The above described PLGA was dissolved in 1,4-dioxane as 3 wt-% solution. The 3 wt-% PLGA solution was immersed into BGf carded mesh, and the samples were frozen to −30°C for 24 hr prior to 24-hr freeze-drying. The freeze-dried PLGA–BGf composites were afterwards cut with a puncher into samples with diameter of 4 mm, and five parallel samples were placed on top of each other and glued together with 3 wt-% PLGA solution and freeze-dried again as described earlier. The height of the final sample was 8 mm, with a porosity of 96% (Haaparanta et al., 2015). The samples were held under vacuum at room temperature for a minimum of 48 hr and gamma sterilized at 25 kGy.

PLGA and PLGA–BGf were compared with two commercial bone substitutes, BG granules (BonAlive®, BonAlive Biomaterials Ltd, Turku, Finland) and β-TCP granules (Synthes® chronOS, Synthes GmbH, Oberdorf, Switzerland), and with spontaneous repair. BonAlive® granules are BG granules consisting of 53 SiO_2, 23 Na_2O, 20 CaO, and 4 P_2O_5 (in wt-%). The BG granules had a diameter of 0.5–0.8 mm. Synthes® chronOS granules are composed of β-TCP. The sizes of these granules were 0.5–0.7 mm, and the porosity of the material was 60%.

2.2 | Surgical procedure

The rabbits were operated under general anaesthesia induced with 0.5 mg/kg (sc) medetomidine and 25 mg/kg (sc) ketamine. Preoperative analgesia of 0.05 mg/kg (sc) of buprenorphine and 4 mg/kg (sc) of carprofen was administered. All the animals received 40 mg/kg (im) of cefuroxime preoperatively.

The animals were set on a supine position on the operating table. A medial parapatellar arthrotomy was made to the right hind leg. The patella was dislocated laterally, and the femoral condyles were exposed. A single lesion through the articular cartilage of the medial condyle was made with a hand-operated drill. The lesion covered almost the width of the femoral condyle, and the bony defect comprised a notable volume of the entire condyle with a diameter of 4 mm and a depth of 8 mm (as depicted in Figure 1b,c). The defect extended into the bone marrow space. The lesions were filled with the studied biomaterial or left empty for spontaneous repair. The granular materials BG and β-TCP were mixed with sterile water to create a paste-like composition prior to implantation. The PLGA and PLGA–BGf samples were semirigid plugs, which were press-fitted into the lesion (Figure 1a). The incisions were closed in layers. After the operation, 1 mg/kg (sc) of antipamexole was administered for reversal of the sedative effects of medetomidine.

The animals were allowed free weight-bearing and unrestricted movement after the operation. Antibiotic prophylaxis of 40 mg/kg (sc) of cefuroxime was continued three times a day for 3 days and postoperative analgesia of 0.01 mg/kg (sc) of buprenorphine and 4 mg/kg (sc) of carprofen for 4 days.

The follow-up time for each group was 12 weeks, whereafter the animals were anaesthetized as described above and euthanized with an overdose of pentobarbital (60 mg/kg, iv). The operated and nonoperated contralateral knees were photographed, evaluated for

gross macroscopic appearance, detached, and stored in 10% buffered formalin at +4°C for further processing.

2.3 | X-ray microtomography

Quantitative analyses of the operated femoral condyles were carried out with X-ray microtomography (μCT) imaging. Bone growth into the lesion and the subchondral bone morphology of the operated and nonoperated contralateral knees were analysed with Zeiss Xradia MicroXCT-400 (Zeiss, Pleasanton, CA, USA). The samples were transferred to the temperature of the μCT device (+29°C) for 30 min before the imaging to stabilize the set-up. The μCT imaging parameters were 100 kV source voltage (no filtering), 100 μA current, 0.4× macro objective, 2 binning, 800 projections, 360° projection angle, and 2.5 s exposure time. The cross-sectional image stacks were reconstructed using Zeiss Xradia XMReconstructor software (version 8.1, Zeiss), resulting in a 22.6-μm isotropic voxel size. The images were postprocessed and visualized using Avizo Fire 8.1 (FEI Visualization Sciences Group, Hillsboro, OR, USA) software. A cylindrical volume of interest (VOI) with a diameter of 5 mm and a depth of 8 mm was extracted. Subsequently, the VOI was denoised with the non-local means (NLM) filter (Buades, Coll, & Morel, 2005). The bone tissue and the implanted biomaterials were segmented by global thresholding. Manual correction was used to reduce segmentation over/under flow.

Quantitative analysis was performed using BoneJ plug-in (Doube et al., 2010) in Fiji (Schindelin et al., 2012) software. The analysed parameters were bone volume fraction (*BV/TV*), trabecular thickness (*Tb.Th*), trabecular spacing (*Tb.Sp*), and trabecular number (*Tb.N*).

2.4 | Histological analysis

The femurs were carefully split into two using a jig saw. Undecalcified samples were dehydrated in ethanol, cleared with xylene immersions, and subsequently embedded in methyl methacrylate. The hardened tissue blocks were cut into 5- to 10-μm thick sections with a Leica SM 2500 hard tissue slide microtome. The sections were stained with Masson–Goldner trichrome stain and mounted with permanent mounting medium. The sections were imaged with a Zeiss AxioImager Z1 microscope system equipped with an AxioCam MRc5 camera and Zen blue edition software (Carl Zeiss Microscopy GmbH, Göttingen, Germany) to acquire mosaic images of the entire histological sections.

For histomorphometry, the Masson–Goldner trichrome stained sections were imaged with an Olympus BX-60 microscope with an integrated Scion colour digital camera. ImageJ software was used for measurements, and scaling was performed with UKAS calibrated auxiliary object glass with a 1-mm scale. Semi-automatic image analysis with ImageJ was used for measuring the total surface area and the trabecular area of the defect. The qualitative assessment of the amount of osteoid and lymphocytes was carried out with the naked eye. Due to the low quantity of osteoid in the samples, quantitative assessment of the amount of osteoid could not be made.

2.5 | Statistical analyses

Relative μCT values, where each parameter for operated knees was compared with the corresponding nonoperated controls, were calculated and used to compare the groups with each other. Statistical analyses were carried out using the permutation analysis of variance test with Holm adjustment. The *p*-values under 0.05 were considered statistically significant.

3 | RESULTS

3.1 | Animal experiment

Three animals (one each from groups PLGA, β-TCP, and spontaneous) died during the induction of anaesthesia, probably due to respiratory arrest caused by the combination of ketamine and medetomidine (Calasans-Maia, Monteiro, Ascoli, & Granjeiro, 2009). Consequently, these three animals were not included in the analyses. Otherwise, the operations were carried out without complications, and all the animals recovered well.

3.2 | Macroscopic appearance

There were no signs of synovitis in the operated joints. All groups showed macroscopic lesion filling up to the joint surface (Figure 2). Repair tissue hypertrophy over the level of the surrounding cartilage was detected in two of eight samples in PLGA–BGf group, in one of six samples in PLGA group, and in one of eight samples in BG group. No overgrowth was detected in the spontaneously healed or in β-TCP-augmented groups. The surface of the neotissue in the defect areas in each group was uneven and differed by colour from healthy cartilage, but no deep tissue deficiencies were detected in the adjacent cartilage.

3.3 | Bone repair

Unresolved β-TCP and BG were still seen in μCT imaging. The bone and biomaterial could both be distinguished from the μCT images in all the test groups. The relative bone volume fraction between the operated and nonoperated knees (Δ*BV/TV*) was greatly increased in the β-TCP group, where it was higher than in the other groups (*p* ≤ 0.012, Figure 3a, Table 1, Table S1). The relative trabecular thickness (Δ*Tb.Th*) was higher in groups PLGA, PLGA–BGf, and spontaneous than in the commercial controls β-TCP and BG (*p* ≤ 0.035; Figure 3b). All groups differed from each other (*p* ≤ 0.048) in relative trabecular spacing (Δ*Tb.Sp*) with the exception of PLGA and spontaneous groups, which did not show a statistical difference from one another (Figure 3c). The trabeculae were sparsest in the PLGA–BGf group (*p* ≤ 0.014).

The trabecular number (*Tb.N*) was close to the contralateral control in the β-TCP and BG groups (Figure 3d). These commercial groups did not differ from one another, but compared with the other groups, their relative trabecular number (Δ*Tb.N*) was significantly higher (*p* ≤ 0.013).
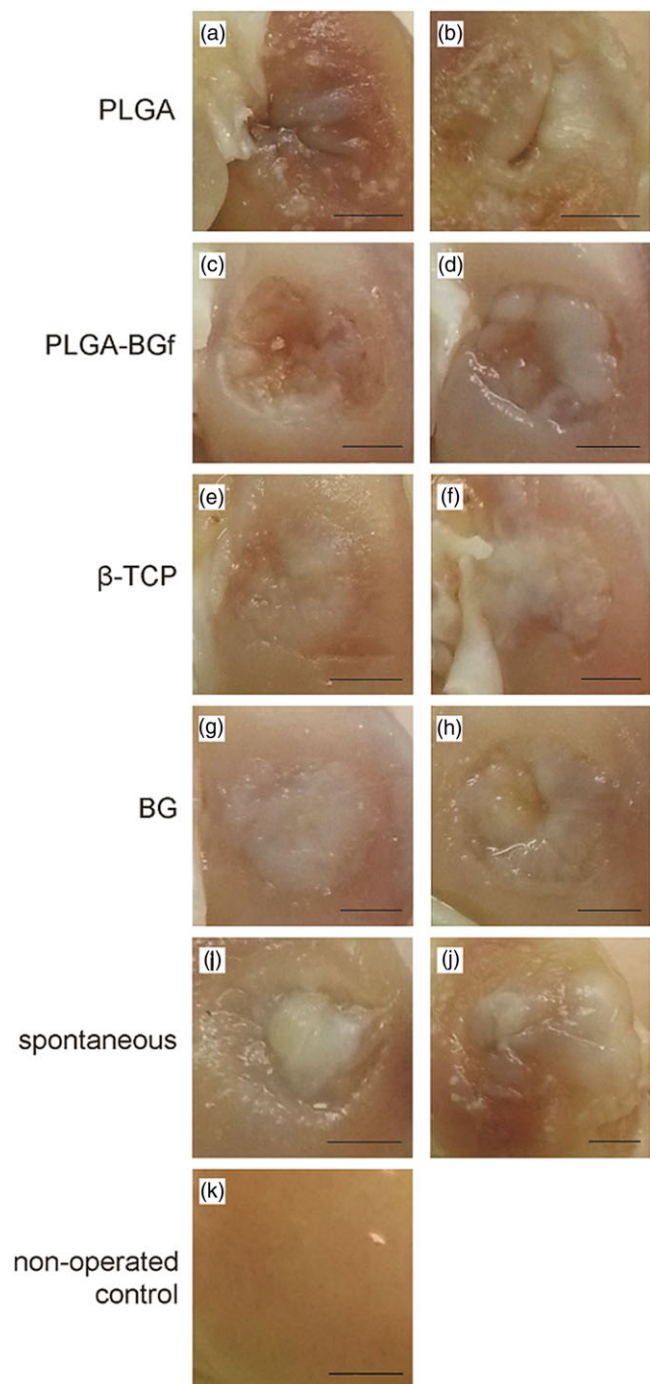
FIGURE 2 Photographs of two representative samples in each group, showing the macroscopic appearance of the cartilage surface where the drill hole was created. The groups are as follows: (a,b) poly(lactide-co-glycolide) (PLGA), (c,d) poly(lactide-co-glycolide)–bioactive glass fibres (PLGA–BGf), (e,f) beta-tricalcium phosphate (β-TCP), (g,h) bioactive glass (BG), (i,j) spontaneous, and (k) a nonoperated contralateral control. Scale bars: 2 mm (a–j) and 5 mm (k) [Colour figure can be viewed at wileyonlinelibrary.com]

Table 1 summarizes the results of the µCT imaging in each group in both the operated knees and the nonoperated contralateral control knees of the same animals. All statistically significant differences in $\Delta BV/TV$, $\Delta Tb.Th$, $\Delta Tb.Sp$, and $\Delta Tb.N$ are presented in Table S1.

3.4 | Repair tissue structure

The filling of the bony lesions seemed to migrate from the edges towards the middle of the defect. Histological assessment of the samples showed that the areas that appear empty in µCT images consist of connective tissue and bone marrow (Figure 4a,b).

In the PLGA and spontaneous groups, the defects were filled partly with fibrous tissue and partly with mineralized bone surrounded by scarce strands of osteoid (Figure 4a,b). The upper halves of the defects were well repaired, but the bone structure in the lower halves was sparse.

In the PLGA–BGf group, the bone defects were filled with fibrous tissue (Figure 4a,b). The perimeter of the defect site featured newly mineralized bone, but the surgically created defect itself showed no bone tissue formation.

Osteoid was seen in most of the samples, where it was located directly beneath the surface. Only one specimen in the spontaneously healed group and one in the PLGA–BGf group had no osteoid (Table 2). Osteoid was most abundant in the β-TCP group, where it encircled numerous small islands of mineralized bone (Figure 4d). Both commercial controls showed comprehensive lesion filling with tissue where mineralized bone and osteoid alternated with cell-rich fibrous tissue. Although the bone defect filling was satisfactory, there was a connective tissue-filled depression near the surface in β-TCP and BG groups (Figure 4a,b).

There was a low number of lymphocytes and macrophages in the histological sections (Table 2). Most inflammatory cells were seen in the PLGA group, where three of seven specimens showed 50–100 inflammatory cells on the slide, and in the PLGA–BGf group, where two of eight specimens showed 50–100 inflammatory cells. No other group showed an increase in the number of lymphocytes or macrophages.

4 | DISCUSSION

In this study, the use of bone defect fillers in intra-articular lesions was evaluated in a rabbit model. Our goal was to find out whether these fillers can be used in repairing the bony part of deep osteochondral defects. As PLGA-based scaffolds have been reported to produce favourable results when used to repair bone defects (Pan et al., 2015; Penk et al., 2013), we hypothesized that creating a rod-like PLGA-based bone filler would enhance the repair of the deep bony part of osteochondral defects and that combining BG with PLGA would further improve the scaffold.

We thought that the PLGA-based semi-rigid bone substitutes might have had additional advantage, as they could be constructed into a two-layer scaffold shaped to match the contours of the joint, with bone substituting material in the deeper part and regenerative cells for cartilage repair in the joint surface. This kind of a scaffold could be used as a bioprosthesis to fill the entire osteochondral defect.

Although the gas-foamed PLGA showed high porosity, the pores were collapsed (Uppstu, Paakki, & Rosling, 2015). As high porosity is needed for bone growth into the scaffold (Zeimaran et al., 2015), this might provide an explanation for the results that were worse than
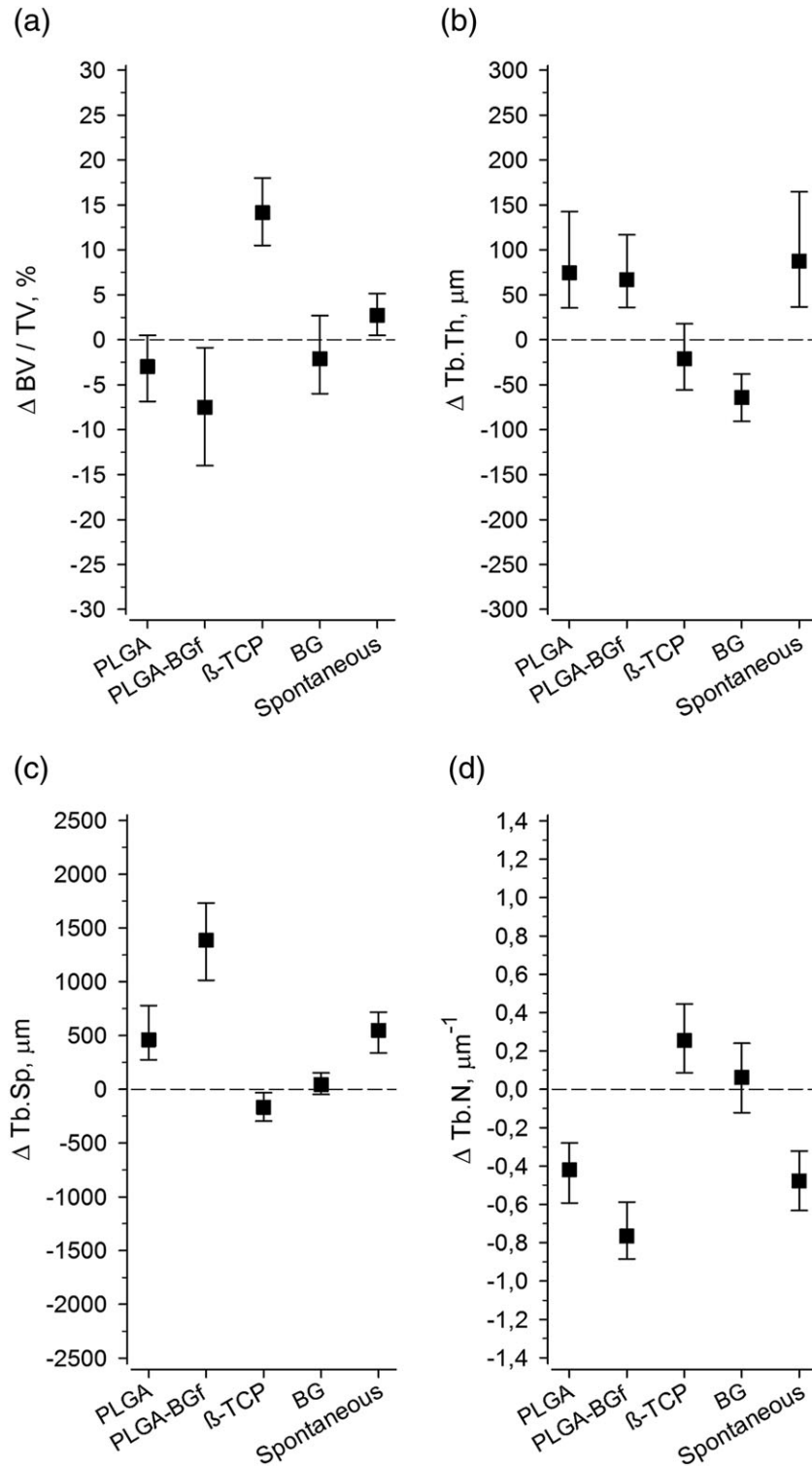
(a)

(b)

(c)

(d)

FIGURE 3 Quantitative results of X-ray microtomography showing the difference between the operated and the nonoperated contralateral knees in (a) bone volume fraction ($\Delta BV/TV$, %), (b) trabecular thickness ($\Delta Tb.Th$, μm), (c) trabecular spacing ($\Delta Tb.Sp$, μm), (d) and trabecular number ($\Delta Tb.N$, μm^{-1}) in each study group. The black square represents the average value of the operated knees, and the dash line represents the nonoperated knees. The whiskers represent 95% confidence intervals

expected. However, the use of gas-foamed PLGA produced repair tissue that did not differ from spontaneous healing, indicating that although it did not have a major overall impact on the healing process, the repair was not hampered by the material.

BG alone has been shown to work well in bone repair (Lindfors, Heikkila, Koski, Mattila, & Aho, 2009) and to promote bone formation in combination with polymers in vitro (Lu, El-Amin, Scott, & Laurencin, 2003). In the present study, BG alone resulted in adequate bone formation, but combining PLGA with BGf deteriorated the repair process. PLGA–BGf had initially small pores and compact structure with very

little space for tissue ingrowth (Haaparanta et al., 2015). The BGfs were densely embedded in the PLGA, which probably impaired the interaction of BGf with the surrounding bone. As the composite material has a longer degradation time than the PLGA alone, it might lead to better structural support in load-bearing applications (Gentile et al., 2014) but delay the lesion repair (Haaparanta et al., 2015). We believe these factors explain why the bone defects treated with the PLGA–BGf composite scaffold were only filled with connective tissue and why the bone structure remained nearly unchanged throughout the 3-month long study period.

TABLE 1 Results of the X-ray microtomography imaging in each group in both the operated knees and the nonoperated contralateral control knees of the same animals

Operated	PLGA Mean ± SE n = 7	PLGA–BGf Mean ± SE n = 8	β-TCP Mean ± SE n = 7	BG Mean ± SE n = 8	Spontaneous Mean ± SE n = 7
BV/TV, %	33.6 ± 1.4	25.1 ± 3.6	46.0 ± 1.3	30.5 ± 1.7	37.1 ± 1.6
Tb.Th (µm)	354 ± 19	295 ± 18	225 ± 10	161 ± 9	364 ± 30
Tb.Sp (µm)	1050 ± 121	1984 ± 178	529 ± 26	632 ± 49	1144 ± 96
Tb.N (µm^{-1})	0.74 ± 0.05	0.46 ± 0.04	1.33 ± 0.04	1.30 ± 0.08	0.68 ± 0.05
Nonoperated	**PLGA** Mean ± SE n = 7	**PLGA–BGf** Mean ± SE n = 8	**β-TCP** Mean ± SE n = 7	**BG** Mean ± SE n = 8	**Spontaneous** Mean ± SE n = 7
BV/TV (%)	36.6 ± 0.8	32.6 ± 0.9	31.9 ± 1.5	32.6 ± 1.3	34.4 ± 2.0
Tb.Th (µm)	280 ± 10	228 ± 9	246 ± 12	226 ± 8	277 ± 19
Tb.Sp (µm)	589 ± 22	597 ± 27	695 ± 45	587 ± 19	595.0 ± 36.0
Tb.N (µm^{-1})	1.16 ± 0.04	1.22 ± 0.05	1.08 ± 0.05	1.24 ± 0.03	1.16 ± 0.05

Note. β-TCP: beta-tricalcium phosphate; BG: bioactive glass; BV/TV: bone volume fraction of the total tissue volume; PLGA: poly(lactide-co-glycolide); PLGA–BGf: poly(lactide-co-glycolide)–bioactive glass fibres; Tb.N, trabecular number; Tb.Sp, trabecular spacing; Tb.Th, trabecular thickness. The values are presented as mean ± standard error (SE).
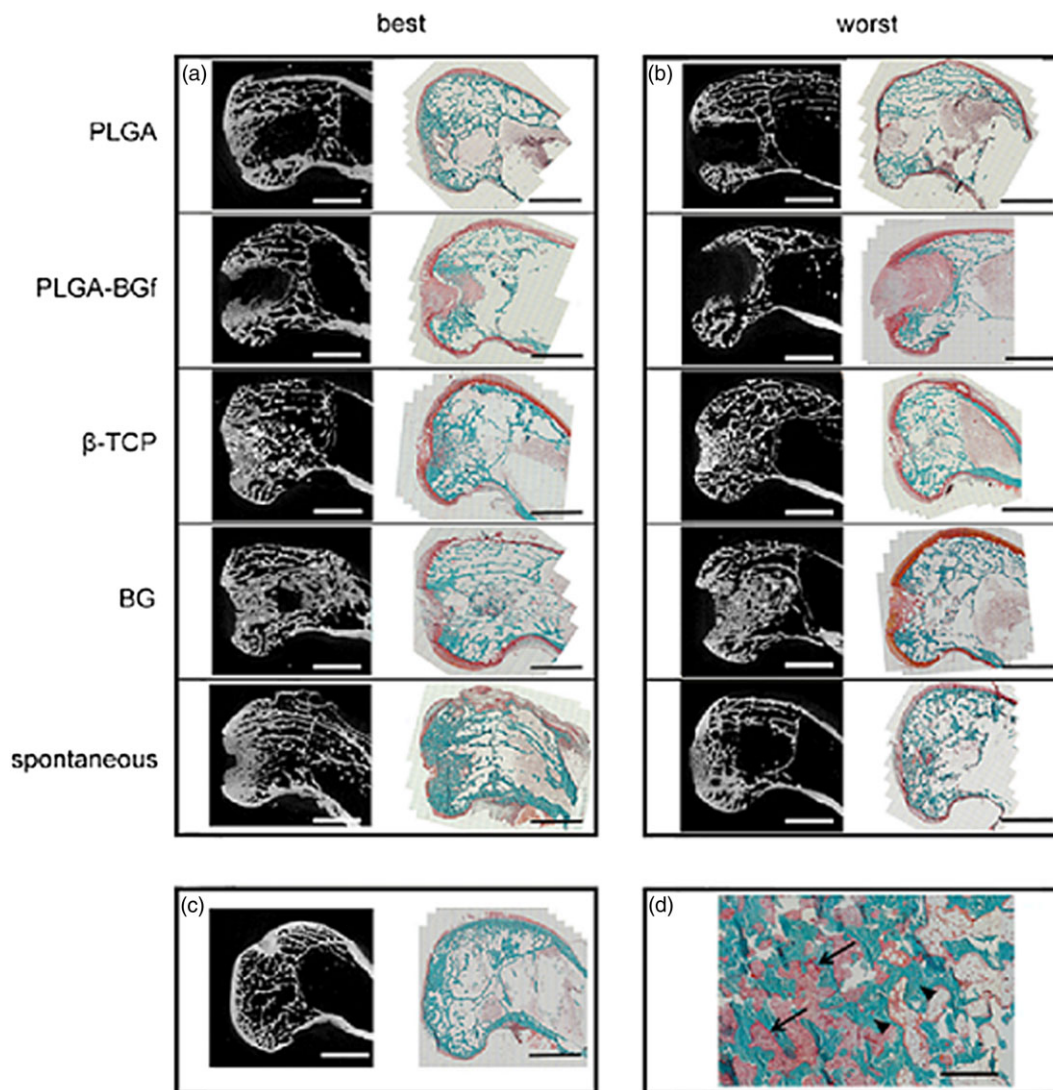

FIGURE 4 An X-ray microtomography (µCT) image and a Masson–Goldner trichrome-stained histological section of (a) the best and (b) the worst sample in each group, chosen according to the data obtained from the µCT imaging, as well as a nonoperated contralateral control (c). The close-up image of the best beta-tricalcium phosphate (β-TCP) section (d) shows the abundance of osteoid (arrow) in the perimeter of the mineralized bone (arrowhead). Scale bars: (a–c): 4 mm, (d) 500 µm [Colour figure can be viewed at wileyonlinelibrary.com]

TABLE 2 Number of animals (*n*) in each study group that presented with abundant, moderate, little, or no osteoid or 0–50, 50–100, and over 500 inflammatory cells in qualitative assessment of histology. None of the samples were classified to have abundant amounts of osteoid. Most inflammatory cells were seen in the PLGA and PLGA–BGf groups

		Osteoid (*n*)				Inflammatory cells (*n*)		
		Abundant	**Moderate**	**Little**	**No osteoid**	**0–50**	**50–100**	**>500**
Group	PLGA (*n* = 7)	0	2	5	0	4	3	0
	PLGA–BGf (*n* = 8)	0	0	7	1	6	2	0
	β–TCP (*n* = 7)	0	3	4	0	7	0	0
	BG (*n* = 8)	0	1	7	0	7	0	0
	spontaneous (*n* = 7)	0	1	5	1	7	0	0

Note. β-TCP: beta-tricalcium phosphate; BG: bioactive glass; PLGA: poly(lactide-co-glycolide); PLGA–BGf: poly(lactide-co-glycolide)–bioactive glass fibres. The values are presented as mean ± standard error (SE).

Degradation of PLGA occurs through hydrolysis, which produces lactic acid and glycolic acid, possibly lowering the pH of its surroundings (Gentile et al., 2014; Haaparanta et al., 2015). The inflammatory reaction and autocatalytic process caused by the acidic environment have been reported to promote bone reparative process (Mountziaris & Mikos, 2008; Zeimaran et al., 2015), although contradicting results have also been presented (Han et al., 2009,Shibutani & Heersche, 1993). In the present study, a slight increase in inflammatory cells was seen in the PLGA and PLGA–BGf-treated specimens but not in the spontaneously healed group or in the groups treated with the granular biomaterials. However, the minor inflammatory reaction seen in the PLGA-based treatment groups did not lead to enhanced bone repair.

In this study, the β-TCP group showed most osteoid, numerous thin trabeculae, and extensive bone formation at 12 weeks. In a previous study in sheep (Mayr et al., 2015), β-TCP resorption and bone formation continued for a long time, with only 12% of the biomaterial being resorbed after 24 weeks. In the present study in rabbits, the 12-week follow-up period shows bone repair in its early phase. It is probable that with time, the bone would have been exposed to remodelling to normalize the trabecular structure.

The bone volume fraction in the operated knees was close to that of the nonoperated controls in the spontaneously healed group. However, the trabeculae were thick and sparse in the spontaneously healed knees, unlike in the groups treated with the commercial granular bone substitutes β-TCP and BG, thus demonstrating a worse healing response than with the granular bone fillers. BG alone showed bone trabecular parameters that were closest to those of the nonoperated contralateral legs, indicating desirable overall repair tissue quality.

The β-TCP granules used in this study have been in clinical use in bone defect repair for over 20 years (Altermatt, Schwobel, & Pochon, 1992). The clinical use of granular β-TCP and BG in osteochondral defect filling, however, has been scanty (Hupa & Hupa, 2010). Granular structure enables easy and complete filling of misshapen osteochondral lesions, without a need to surgically enlarge the lesion to fit the shape of the scaffold. Granular bone fillers allow cell migration into the entire defect site, tissue ingrowth, vascularization, and well-functioning metabolism (Virolainen, Heikkila, Yli-Urpo, Vuorio, & Aro, 1997; Zerbo, Bronckers, de Lange, & Burger, 2005). In this study, the commercial materials BG and β-TCP showed satisfactory lesion filling and extensive bone formation, indicating that they have potential

to be used in deep osteochondral defect repair. The potential downside of granular materials is that the granules might loosen from the surface. However, in this study, the articulating tibial surface showed no signs of abrasion by the granules. Adding a cartilage reparative scaffold on top of the bone repair would further secure the granules in place while restoring the cartilage surface.

There is emerging evidence of crosstalk between articular cartilage and underlying subchondral bone that emphasizes the importance of restoring the joint as a unit (Findlay & Kuliwaba, 2016). Survival of a whole tissue graft in osteochondral grafting depends largely on the integration of the graft bone into the host bone (Gross et al., 2008). Despite the favourable bone repair with the commercial bone substitute materials, the cartilage unit of the defect, which was left untreated, was inadequately repaired in the present study. Even though Masson–Goldner trichrome is not a cartilage staining method, it gives a general view of the tissue repair. For the tissue section analysed in the present study for detailed bone formation, it was evident that there was no or very minor cartilage formation over the bone regrowth. Thus, none of the studied materials alone were sufficient for the restoration of the entire osteochondral unit. Similar results were obtained in a study where PLGA was combined with hydroxyapatite-β-TCP (Fan et al., 2013) and in the work of Matsuo and colleagues (Matsuo et al., 2015) in which osteochondral repair was studied in a minipig model. A separate cartilage repair procedure on top of bone repair is therefore needed to restore the chondral part of the lesion.

The strength of this study is in its comparison of four different bone fillers with each other and with spontaneous repair. The bone defects were very large, creating a challenge both for the spontaneous repair and for the treatment groups. This study was limited by the lack of a healthy age-adjusted control group with no surgical procedures. In this study, it is possible that the operated limb carried less weight than the contralateral control limb. However, this animal-specific control was the same for every group, enabling comparison between the study groups.

5 | CONCLUSIONS

Filling of the bony part of a deep osteochondral lesion with a biodegradable gas-foamed PLGA scaffold resulted in insufficient repair. Combining PLGA with bioactive glass worsened the repair result.

The commercial controls with β-TCP and BG resulted in satisfactory bone defect filling with more abundant osteoid and mineralized bone tissue. Thus, these two bone substitute materials have the potential to be used in deep osteochondral defect repair, given that the cartilage unit of the defect is repaired with adequate techniques.

ACKNOWLEDGEMENTS

CONFLICT OF INTEREST

The authors have no financial or personal disclosures that would pose potential conflicts of interests.

AUTHOR CONTRIBUTIONS

Conception and design of the study: V.M., E.J., A.R., M.K., I.K.; providing study materials: P.U., A.M.H., A.R., M.K.; acquisition of data: E.S., V. M., K.L., E.J., T.P., M.H.; analysis and interpretation of data: E.S., V.M., K.L., M.H., A.A., I.K.; drafting the article: E.S., V.M., K.L., E.J., T.P., M.H., P.U., A.M.H.; critical revision of the article for important intellectual content: A.A., A.R., M.K., I.K.

All authors have read and approved the final submitted manuscript.

ORIGINAL PUBLICATION

This manuscript contains original unpublished work and it is not being submitted for publication elsewhere at the same time.

ORCID

Eve Salonius https://orcid.org/0000-0003-1988-2800

REFERENCES

Altermatt, S., Schwobel, M., & Pochon, J. P. (1992). Operative treatment of solitary bone cysts with tricalcium phosphate ceramic. A 1 to 7 year follow-up. *European Journal of Pediatric Surgery*, *2*, 180–182. https://doi.org/10.1055/s-2008-1063435

Arrington, E. D., Smith, W. J., Chambers, H. G., Bucknell, A. L., & Davino, N. A. (1996). Complications of iliac crest bone graft harvesting. *Clinical Orthopaedics and Related Research*, *329*, 300–309. https://doi.org/10.1097/00003086-199608000-00037

Brauer, D. S. (2015). Bioactive glasses-structure and properties. *Angewandte Chemie (International Ed. in English)*, *54*, 4160–4181. https://doi.org/10.1002/anie.201405310

Buades, A., Coll, B., & Morel, J. M. (2005). A non-logical algorithm for image denoising. *Computer Vision and Pattern Recognition*, *2*, 60–65.

Calasans-Maia, M. D., Monteiro, M. L., Ascoli, F. O., & Granjeiro, J. M. (2009). The rabbit as an animal model for experimental surgery. *Acta Cirúrgica Brasileira*, *24*, 325–328. https://doi.org/10.1590/S0102-86502009000400014

Doube, M., Klosowski, M. M., Arganda-Carreras, I., Cordelieres, F. P., Dougherty, R. P., Jackson, J. S., ... Shefelbine, S. J. (2010). BoneJ: Free and extensible bone image analysis in ImageJ. *Bone*, *47*, 1076–1079. https://doi.org/10.1016/j.bone.2010.08.023

Eggli, P. S., Muller, W., & Schenk, R. K. (1988). Porous hydroxyapatite and tricalcium phosphate cylinders with two different pore size ranges implanted in the cancellous bone of rabbits. A comparative histomorphometric and histologic study of bony ingrowth and implant substitution. *Clinical Orthopaedics and Related Research*, *232*, 127–138.

Fan, W., Wu, C., Miao, X., Liu, G., Saifzadeh, S., Sugiyama, S., ... Xiao, Y. (2013). Biomaterial scaffolds in cartilage-subchondral bone defects influencing the repair of autologous articular cartilage transplants. *Journal of Biomaterials Applications*, *27*, 979–989. https://doi.org/10.1177/0885328211431310

Findlay, D. M., & Kuliwaba, J. S. (2016). Bone–cartilage crosstalk: A conversation for understanding osteoarthritis. *Bone Research*, *4*, 16028. https://doi.org/10.1038/boneres.2016.28

Garcia-Gareta, E., Coathup, M. J., & Blunn, G. W. (2015). Osteoinduction of bone grafting materials for bone repair and regeneration. *Bone*, *81*, 112–121. https://doi.org/10.1016/j.bone.2015.07.007

Gentile, P., Chiono, V., Carmagnola, I., & Hatton, P. V. (2014). An overview of poly (lactic-co-glycolic) acid (PLGA)-based biomaterials for bone tissue engineering. *International Journal of Molecular Sciences*, *15*, 3640–3659. https://doi.org/10.3390/ijms15033640

Ghazal, G., Prein, J., & Müller, W. (1992). Knochendefektfüllungen in den Kieferknochen mit Tricalciumphosphat. *Swiss Dent*, *13*, 15–18.

Gross, A. E., Kim, W., Las Heras, F., Backstein, D., Safir, O., & Pritzker, K. P. (2008). Fresh osteochondral allografts for posttraumatic knee defects: Long-term followup. *Clinical Orthopaedics and Related Research*, *466*, 1863–1870. https://doi.org/10.1007/s11999-008-0282-8

Gunn, J. M., Rekola, J., Hirvonen, J., & Aho, A. J. (2013). Comparison of the osteoconductive properties of three particulate bone fillers in a rabbit model: Allograft, calcium carbonate (Biocoral(R)) and S53P4 bioactive glass. *Acta Odontologica Scandinavica*, *71*, 1238–1242. https://doi.org/10.3109/00016357.2012.757642

Haaparanta, A. M., Uppstu, P., Hannula, M., Ella, V., Rosling, A., & Kellomaki, M. (2015). Improved dimensional stability with bioactive glass fibre skeleton in poly (lactide-co-glycolide) porous scaffolds for tissue engineering. *Materials Science & Engineering. C, Materials for Biological Applications*, *56*, 457–466. https://doi.org/10.1016/j.msec.2015.07.013

Han, S. H., Chae, S. W., Choi, J. Y., Kim, E. C., Chae, H. J., & Kim, H. R. (2009). Acidic pH environments increase the expression of cathepsin B in osteoblasts: The significance of ER stress in bone physiology. *Immunopharmacology and Immunotoxicology*, *31*, 428–431. https://doi.org/10.1080/08923970902751651

Huey, D. J., Hu, J. C., & Athanasiou, K. A. (2012). Unlike bone, cartilage regeneration remains elusive. *Science*, *338*, 917–921. https://doi.org/10.1126/science.1222454

Hupa, L., & Hupa, M. (2010). Recent research on composition dependence of the properties of bioactive glasses. *Ceramic Transactions (Advances in Bioceramics and Biotechnologies)*, *218*, 145–156.

Jackson, D. W., Lalor, P. A., Aberman, H. M., & Simon, T. M. (2001). Spontaneous repair of full-thickness defects of articular cartilage in a goat model. A preliminary study. *Journal of Bone and Joint Surgery-American*, *83-A*, 53–64.

Jones, J. R. (2013). Review of bioactive glass: From Hench to hybrids. *Acta Biomaterialia*, *9*, 4457–4486. https://doi.org/10.1016/j.actbio.2012.08.023

Karp, J. M., Shoichet, M. S., & Davies, J. E. (2003). Bone formation on two-dimensional poly (DL-lactide-co-glycolide) (PLGA) films and three-dimensional PLGA tissue engineering scaffolds in vitro. *Journal of Biomedical Materials Research. Part a*, *64*, 388–396. https://doi.org/10.1002/jbm.a.10420

Keranen, P., Moritz, N., Alm, J. J., Ylanen, H., Kommonen, B., & Aro, H. T. (2011). Bioactive glass microspheres as osteopromotive inlays in macrotextured surfaces of Ti and CoCr alloy bone implants: Trapezoidal surface grooves without inlay most efficient in resisting torsional forces. *Journal of the Mechanical Behavior of Biomedical Materials*, *4*, 1483–1491. https://doi.org/10.1016/j.jmbbm.2011.05.018

Kleinschmidt, J. C., Marden, L. J., Kent, D., Quigley, N., & Hollinger, J. O. (1993). A multiphase system bone implant for regenerating the calvaria. *Plastic and Reconstructive Surgery*, *91*, 581–588. https://doi.org/10.1097/00006534-199304000-00002

Lindfors, N. C., Heikkila, J. T., Koski, I., Mattila, K., & Aho, A. J. (2009). Bioactive glass and autogenous bone as bone graft substitutes in benign bone tumors. *Journal of Biomedical Materials Research. Part B, Applied Biomaterials*, *90*, 131–136.

Lindfors, N. C., Hyvonen, P., Nyyssonen, M., Kirjavainen, M., Kankare, J., Gullichsen, E., & Salo, J. (2010). Bioactive glass S53P4 as bone graft substitute in treatment of osteomyelitis. *Bone*, *47*, 212–218. https://doi.org/10.1016/j.bone.2010.05.030

Liu, B., & Lun, D. X. (2012). Current application of beta-tricalcium phosphate composites in orthopaedics. *Orthopaedic Surgery*, *4*, 139–144. https://doi.org/10.1111/j.1757-7861.2012.00189.x

Lu, H. H., El-Amin, S. F., Scott, K. D., & Laurencin, C. T. (2003). Three-dimensional, bioactive, biodegradable, polymer-bioactive glass composite scaffolds with improved mechanical properties support collagen synthesis and mineralization of human osteoblast-like cells in vitro. *Journal of Biomedical Materials Research. Part a*, *64*, 465–474. https://doi.org/10.1002/jbm.a.10399

Mano, J. F., & Reis, R. L. (2007). Osteochondral defects: Present situation and tissue engineering approaches. *Journal of Tissue Engineering and Regenerative Medicine*, *1*, 261–273. https://doi.org/10.1002/term.37

Matsuo, T., Kita, K., Mae, T., Yonetani, Y., Miyamoto, S., Yoshikawa, H., & Nakata, K. (2015). Bone substitutes and implantation depths for subchondral bone repair in osteochondral defects of porcine knee joints. *Knee Surgery, Sports Traumatology, Arthroscopy*, *23*, 1401–1409. https://doi.org/10.1007/s00167-014-2853-4

Mayr, H. O., Suedkamp, N. P., Hammer, T., Hein, W., Hube, R., Roth, P. V., & Bernstein, A. (2015). beta-Tricalcium phosphate for bone replacement: Stability and integration in sheep. *Journal of Biomechanics*, *48*, 1023–1031. https://doi.org/10.1016/j.jbiomech.2015.01.040

McKinley, T. O., Borrelli, J. Jr., D'Lima, D. D., Furman, B. D., & Giannoudis, P. V. (2010). Basic science of intra-articular fractures and posttraumatic osteoarthritis. *Journal of Orthopaedic Trauma*, *24*, 567–570. https://doi.org/10.1097/BOT.0b013e3181ed298d

Mountziaris, P. M., & Mikos, A. G. (2008). Modulation of the inflammatory response for enhanced bone tissue regeneration. *Tissue Engineering. Part B, Reviews*, *14*, 179–186. https://doi.org/10.1089/ten.teb.2008.0038

Oryan, A., Alidadi, S., Moshiri, A., & Maffulli, N. (2014). Bone regenerative medicine: Classic options, novel strategies, and future directions. *Journal of Orthopaedic Surgery and Research*, *9*, 18. 799X-9-18, DOI: https://doi.org/10.1186/1749-799X-9-18

Pan, Z., Duan, P., Liu, X., Wang, H., Cao, L., He, Y., … Ding, J. (2015). Effect of porosities of bilayered porous scaffolds on spontaneous osteochondral repair in cartilage tissue engineering. *Regenerative Biomaterials*, *2*, 9–19. https://doi.org/10.1093/rb/rbv001

Penk, A., Forster, Y., Scheidt, H. A., Nimptsch, A., Hacker, M. C., Schulz-Siegmund, M., … Huster, D. (2013). The pore size of PLGA bone implants determines the de novo formation of bone tissue in tibial head defects in rats. *Magnetic Resonance in Medicine*, *70*, 925–935. https://doi.org/10.1002/mrm.24541

Schindelin, J., Arganda-Carreras, I., Frise, E., Kaynig, V., Longair, M., & Pietzsch, T. (2012). Fiji: An open-source platform for biological-image analysis. *Nature Methods*, *9*, 676–682. https://doi.org/10.1038/nmeth.2019

Seo, S. J., Mahapatra, C., Singh, R. K., Knowles, J. C., & Kim, H. W. (2014). Strategies for osteochondral repair: Focus on scaffolds. *Journal of Tissue Engineering*, *5*. 2041731414541850 DOI: https://doi.org/10.1177/2041731414541850

Serino, G., Rao, W., Iezzi, G., & Piattelli, A. (2008). Polylactide and polyglycolide sponge used in human extraction sockets: Bone formation following 3 months after its application. *Clinical Oral Implants Research*, *19*, 26–31.

Shibutani, T., & Heersche, J. N. (1993). Effect of medium pH on osteoclast activity and osteoclast formation in cultures of dispersed rabbit osteoclasts. *Journal of Bone and Mineral Research*, *8*, 331–336. https://doi.org/10.1002/jbmr.5650080310

Stahl, S. S., & Froum, S. (1986). Histological evaluation of human intraosseous healing responses to the placement of tricalcium phosphate ceramic implants. I. Three to eight months. *Journal of Periodontology*, *57*, 211–217. https://doi.org/10.1902/jop.1986.57.4.211

Uppstu, P., Paakki, C., & Rosling, A. (2015). In vitro hydrolysis and magnesium release of poly(d,l-lactide-co-glycolide)-based composites containing bioresorbable glasses and magnesium hydroxide. *Journal of Applied Polymer Science*, *132*, 41. 42646

van Dijk, C. N., Reilingh, M. L., Zengerink, M., & van Bergen, C. J. (2010). Osteochondral defects in the ankle: Why painful? *Knee Surgery, Sports Traumatology, Arthroscopy*, *18*, 570–580. https://doi.org/10.1007/s00167-010-1064-x

Virolainen, P., Heikkila, J., Yli-Urpo, A., Vuorio, E., & Aro, H. T. (1997). Histomorphometric and molecular biologic comparison of bioactive glass granules and autogenous bone grafts in augmentation of bone defect healing. *Journal of Biomedical Materials Research*, *35*, 9–17. https://doi.org/10.1002/(SICI)1097-4636(199704)35:1<9::AID-JBM2>3.0.CO;2-S

Zeimaran, E., Pourshahrestani, S., Djordjevic, I., Pingguan-Murphy, B., Kadri, N. A., & Towler, M. R. (2015). Bioactive glass reinforced elastomer composites for skeletal regeneration: A review. *Materials Science & Engineering. C, Materials for Biological Applications*, *53*, 175–188. https://doi.org/10.1016/j.msec.2015.04.035

Zerbo, I. R., Bronckers, A. L., de Lange, G., & Burger, E. H. (2005). Localisation of osteogenic and osteoclastic cells in porous beta-tricalcium phosphate particles used for human maxillary sinus floor elevation. *Biomaterials*, *26*, 1445–1451. https://doi.org/10.1016/j.biomaterials.2004.05.003

SUPPORTING INFORMATION

Additional supporting information may be found online in the Supporting Information section at the end of the article.

Table S1. Quantitative results of X-ray microtomography showing all statistically significant p values ($p \leq 0.05$) obtained with a permutation ANOVA test with Holm adjustment.